JOURNAL OF SOLID STATE CHEMISTRY **52**, 274–280 (1984)

Crystal Structures and Phase Transition of Rb_2TeBr_6 (300–12.5 K)

W. ABRIEL*

Sonderforschungsbereich 127 und Fachbereich Chemie der Universität, Lahnberge, D-3550 Marburg, Federal Republic of Germany

AND J. IHRINGER

Institut für Kristallographie der Universität, Charlottenstr. 33, D-7400 Tübingen, Federal Republic of Germany

Received July 19, 1983; in revised form October 24, 1983

Using 298 and 160(3) K diffractometer intensity data the structure of Rb_2TeBr_6 has been determined by single crystal X-ray technique and refined to a final R_w of 0.041 and 0.037, respectively (K_2PtCl_6 type structure, space group $Fm3m$, $Z = 4$ with $a_{298} = 10.773(4)$ Å and $a_{160} = 10.713(6)$ Å). The powder diffraction pattern from 300 to 12.5 K was recorded by a low-temperature Guinier diffractometer and camera. Below 45(5) K a second-order phase transition leads to a tetragonally distorted structure corresponding to a softening of the $T_{1g}(\Gamma)$ rotary phonon. The powder pattern measured with the diffractometer at 12.5 K was used for structural refinement ($R = 0.092$). This low-temperature phase shows a ferrorotative displacement of the $TeBr_6$-octahedra with a tilt angle of 4.7(1) deg. (space group $I4/m$, $Z = 2$, $a = 7.4726(3)$ Å and $c = 10.7008(5)$ Å). The structural results indicate that there is no stereochemical activity of the lone pair electrons at Te(IV) even at very low temperatures. Phase transitions of Rb_2TeBr_6 and Rb_2TeI_6 ($A_{2g}(X)$-condensation) are compared. The results of a lattice dynamic calculation shows that only the $T_{1g}(\Gamma)$ condensation can be explained with a rigid ion model.

Introduction

In 1957 Gillespie and Nyholm (*1*) predicted that hexa-coordinated complexes of Te(IV) should not possess a regular octahedral structure but rather one based on seven coordination with a lone pair of electrons occupying the seventh position. However, all structures so far reported, picking compounds A_2TeBr_6 with A = K, NH_4, Rb, Cs, $(CH_3)_4N$ (*2–5*), for example, indicate that such complexes are in fact regular octahedra. As all these structural investigations were carried out at room temperature, a stereochemical effect of the lone pair electrons at lower temperatures could be possible.

For compounds A_2TeBr_6 (with A = K, NH_4, Rb, Cs) the high-temperature phases show the cubic K_2PtCl_6-type structure (Fig. 1). Lowering the temperature, second-order phase transitions can be observed, especially when the anions are comparatively large. These phase transitions can be explained by a softening of rotary phonons. Generally, in A_2MX_6 compounds this instability is result of a double minimum in the Coulomb potential with respect to the octahedra tilt angle φ around (0 0 1); the depth of this minimum depends on the interaction

---

* To whom correspondence should be addressed. Present address: Institut für Anorganische Chemie der Universität, Callinstrasse 9, D-3000 Hannover, FRG.

0022-4596/84 $3.00

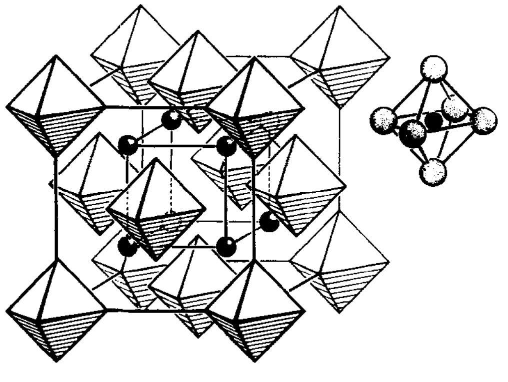

FIG. 1. K_2PtCl_6 structure (from (6)); small spheres K; octahedra $PtCl_6$.

and the radii of the corresponding ions (7).

Table I shows the known phase transitions for some compounds A_2TeBr_6. Lowering the temperature, the first transition leads to a tetragonally distorted structure, space group *P*4/*mnc*, indicating a condensation of the $A_{2g}(X)$ librational mode (A = K, NH_4. As a result of antiferrorotative tilted TeX_6-octahedra, this structure is stable for Rb_2TeI_6 at room temperature (*11*).

Related compounds like Elpasolites (Rb_2NaHoF_6, for example, Ref. (*12*)) show a phase transition corresponding to a softening of the $T_{1g}(\Gamma)$ rotary phonon (ferrorotative-tilted HoF_6-octahedra). From the lattice dynamical point of view, the knowledge of the cause for these different kinds of symmetry reduction should be desirable. A discussion of the results of this low-temperature investigation of Rb_2TeBr_6 in comparison with the data from a Rb_2TeI_6 study (*11*) will give us a hint for understanding the lattice dynamics of A_2MX_6 phases.

Experimental

Crystals of Rb_2TeBr_6 precipitated from a equimolar solution of TeO_2 and Rb_2CO_3 in conc. hydrobromic acid. Weissenberg and precession photographs from a cubeoctahedral single crystal (V = 0.003 mm^3), embedded in adhesive in order to protect it from moisture, showed F-centered Laue symmetry $m\bar{3}m$ according to the crystal symmetry of the K_2PtCl_6-type structure. A Guinier photograph of the powder (Huber Guinier System 600, Ge-standard with a = 5.65775 Å) at 298 K agreed with the lattice parameters found from the single crystal. A least-squares refinement of the lattice dimension yielded the final value using the powder data recorded by film methods. Single crystal intensity measurements of the $Fm3m$ structure at 298 and 160(3) K were performed on a CAD4 diffractometer (Enraf Nonius) using graphite-monochromatized Mo$K\alpha$ radiation in an Ω scan mode (scan angle 2.5°, scan time max. 90 sec with $\theta_{max.} = 30°$). The lattice dimension at 160 K was calculated from 21 reflexions in the range $10° < \theta < 24°$ centered by the diffractometer. Severe absorption effects (μ = 286 cm^{-1}) required the application of numerical absorption corrections limited by the accuracy of crystal size measurement. For the structural calculations the program system

TABLE I

SPACE GROUPS FOR COMPOUNDS A_2TeBr_6 AT DIFFERENT TEMPERATURES

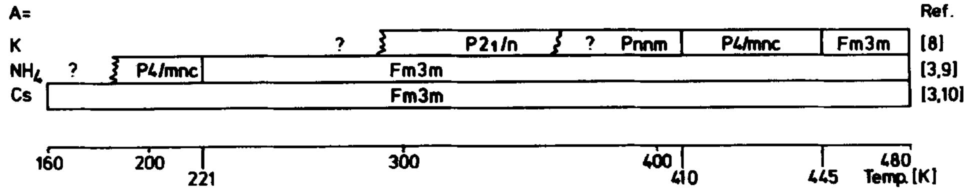

TABLE II

SOME DETAILS FROM THE SINGLE CRYSTAL INVESTIGATIONS. R_{int} SHOWS THE CONSISTENCY IN THE F-VALUES OF EQUIVALENT REFLEXIONS. $R_W = \Sigma\Delta F\sqrt{W}/\Sigma F_0\sqrt{W}$; $R_G = [\Sigma W(\Delta F)^2]^{1/2}/[\Sigma W(F_0)^2]^{1/2}$

Temp. [K]	Measured reflexions	Unique refl. $F > \sigma(F)$	R_{int}	R	R_W	R_G	Weight
298	636	118	0.052	0.06	0.041	0.037	$1.588/\sigma^2(F)$
160(3)	530	117	0.056	0.05	0.037	0.032	$1.161/\sigma^2(F)$

SHELX76 (*13*) was applied using the scattering factors for Rb^+, Te, and Br (from the International Tables (*14*)) considering the anomalous dispersion corrections according to Cromer and Libermann (*15*). Some details from the structure analysis can be taken from Table II.

A powder with particle size less than 50 μm prepared by crushing single crystals was sieved on a silicone-moistened 0.02-mm-thick Mylar foil. The measurements in a temperature range from 300 to 12.5 K were performed with the low-temperature Guinier diffractometer and camera (*16*) with Ge-monochromator and Cu*K*α1 radiation from a rotating anode generator. For a qualitative survey the diffraction pattern (Fig. 2) was recorded at continuously varying temperatures with the film lift device. For the Rietveld refinement (*17*) 1952 intensities ($6.96° \leqq \theta \leqq 46.00°$, step size $0.02°\theta$, measuring time 20 sec at each step) were collected with the diffractometer at 12.5 K. The background substraction in the preparation program based on a linear interpolation between 33 background values selected from a plot of the diagram. In the refinement with formfactors corrected for f′ and f″ (see above) all possible atomic coordinates and the isotropic thermal parameters were varied besides the 6 profile and cell parameters. So the total number of free parameters was 15 for *I*4/*m*, e.g. The single reflexion recordings were prepared by fitting one or more Gaussian or Lorentzian profiles to the measured line shapes. The lattice constants at 12.5 K were evaluated by the Rietveld program.

Results

The parameters found from the single crystal data at 298 and 160(3) K are listed in Table III. A correction of the positional parameter of the Br-atom was applied for the apparent shortening of the Te–Br bond due to thermal motion (*18*) on the assumption that the rigid $TeBr_6^{2-}$-ion is librating about the central tellurium atom. The new parameters were calculated to $x = 0.2510(3)$ at 298 K and $x = 0.2519(2)$ at 160(3) K. The correctness of the rigid ion model can be checked by calculating a generalized *R*-index for the agreement of observed and cal-

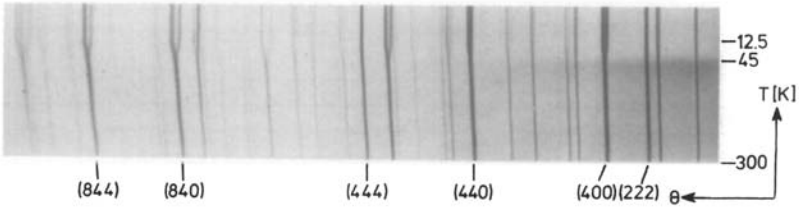

FIG. 2. Guinier diffraction pattern, 300–12.5 K.

TABLE III

Final Parameters for Rb_2TeBr_6 at 298 and 160(3) K (× 10^4). Space Group $Fm3m$, $Z = 4$ with a = 10.773(4) Å at 298 K and a = 10.713(6) Å at 160(3) K. Te in $4a$ (0,0,0); Rb in $8c$ (¼,¼,¼); Br in $24e$ (x,0,0)

Temp. [K]	Te U_{11}	Rb U_{11}	Br x	Br U_{11}	Br U_{22}
298	180(7)	499(11)	2496(2)	190(11)	600(10)
160(3)	87(6)	281(9)	2510(2)	109(10)	356(7)

culated U_{ij} (program XANADU (*19*), R_G = 0.007, and 0.028 at 298 and 160 K, respectively). The final maximum peak height from a $F_0 - F_c$ Fourier map was 7 electrons $Å^{-3}$ in the position (0,0,0) at both temperatures.

The splitting of the cubic reflexions at T_c = 45(5) K (see Fig. 2) leads to a continuously increasing tetragonal lattice distortion. The change of the lattice constants and intensities at T_c is continuous, so the phase transition is of second-order. No further change of symmetry is found between T_c and 12.5 K.

The possible low-temperature space group is therefore the result of a soft mode Γ-point condensation (see also a recent paper of Ihringer (*12*)). Figure 3 displays all possible space groups resulting from a second-order phase transition with $\underset{\sim}{k} = 0$. Each normal mode displacement transforms under the symmetry of $m3m$ according to the irreducible representation in the head of the table. However, in each representation—except A_{1g}—there are symmetries that transform the displacements not in itself, just those symmetries are lost below T_c. So the remaining elements define the space group after the softening of the normal mode. Therefore for the profile refinement the competing space groups $I4/mmm$, $I4mm$, $I\bar{4}2m$, and $I4/m$ were taken into account. The line profile refinement of the 12.5 K diffraction pattern yielded the best

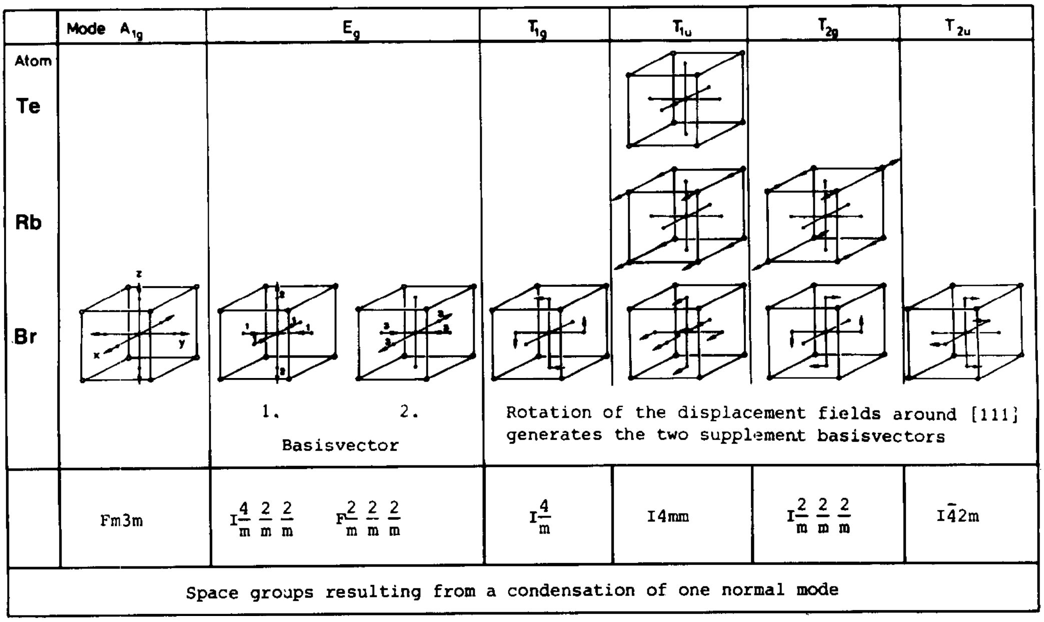

FIG. 3. Normal mode displacement fields in Rb_2TeBr_6.

TABLE IV

FINAL PARAMETERS FOR Rb_2TeBr_6 AT 12.5 K. SPACE GROUP $I4/m$, $Z = 2$ WITH $a = 7.4726(3)$ Å AND $c = 10.7008(5)$ Å

Atom	Position	x	y	z	B [Å^2]
Te	$2a$	0	0	0	0.5(1)
Rb	$4d$	0	$\frac{1}{2}$	$\frac{1}{4}$	0.8(1)
Br(1)	$4e$	0	0	0.2509(6)	0.7(2)
Br(2)	$8h$	0.2341(7)	0.2756(7)	0	1.2(1)

residuals[1] $R = 0.092$, $R_P = 0.19$, and $R_{PW} = 0.20$ for the model $I4/m$ (structural parameters see Table IV).[2] The best of the final residuals for the competing space groups was $R = 0.106$, but while the coordinates in the refinement of the $I4/m$-structure reached their final values after 4 cycles, in the other models they oscillated around their starting values in the limits of 3 σ. We so conclude that the minimum found for $I4/m$ describes the reality.

The interatomic distances are listed in Table V using the corrected positional parameters for Br at 298 and 160 K.

Discussion

An octahedral coordination for the $TeBr_6^{2-}$-ion even at 12.5 K is the most important result from the chemical point of view. The small differences of the Te–Br bond lengths in the low temperature structure are not significant considering the standard deviations and are typical for a tetragonal refinement of positional parameters. So the point symmetry of the $TeBr_6^{2-}$-ion is still $m3m$. There appears to be no stereochemical active lone pair of electrons at Te(IV) in this hexahalo complex ion.

Finally, the phase transition is result of a ferrorotative displacement of the $TeBr_6^{2-}$ octahedra (tilt angle 4.7(1)°) corresponding to a softening of the $T_{1g}(\Gamma)$ rotary phonon. The symmetry of the condensing mode depends on the group–subgroup relations of the space groups when Landau's law is realized *(20)*.

Retaining the cubic structure and the bond distances within the $TeBr_6$-octahedron, the other interatomic distances decrease when cooling from 298 to 160 K. The atomic and molecular motions are diminishing. So a closer contact of the Br atoms between the anions is possible. Below T_c

TABLE V

INTERATOMIC DISTANCES (Å)

Temp. [K]	Te–Br	Br–Br Within anion	Br–Br Between anion	Rb–Br	Rb–Te
1. For Rb_2TeBr_6 at different temperatures					
298	2.704(3)	3.824(3)	3.794(3)	3.809(2)	4.665(2)
160	2.699(2)	3.816(2)	3.759(2)	3.788(2)	4.639(2)
12.5	2.696(6)	3.815(7)	3.701(7)	3.754(3)	4.595(1)

2. For the 12.5 K structure in detail

Te –Br(1)	2x 2.685(7)	
–Br(2)	4x 2.702(5)	
Br(1)–Br(2)	2x 3.809(6)	Within anion
Br(2)–Br(2)	2x 3.821(7)	
Br(2)–Br(2)	2x 3.677(7)	Between anions
Br(1)–Br(2)	2x 3.724(6)	
Rb –Br(1)	4x 3.736(1)	
–Br(2)	4x 3.610(4)	
–Br(2)	4x 3.917(4)	

[a] For the 12.5 K structure the mean values are given.

---

[1] $R = \Sigma_i\ [F_i^2(\text{obs}) - (1/c)F_i^2(\text{calc})]/\Sigma_i\ F_i^2(\text{obs})$; $R_P = \Sigma_i\ [y_i(\text{obs}) - y_i(\text{calc})]^2/\Sigma_i\ [y_i(\text{obs})]^2$; $R_{PW} = \Sigma_i\ w_i[y_i(\text{obs}) - y_i(\text{calc})]^2/\Sigma_i\ w_i[y_i(\text{obs})]^2$. The reason for the relative high profile residuals lies in the insufficient corrections for the asymetric line shapes at low angles.

[2] Tables of observed and calculated structure factors and the $F^2(\text{obs})/F^2(\text{calc})$- listing from the Rietveld refinement of the powder data as well as the raw profile data are deposited with the National Auxiliary Publications Service. See NAPS document No. 04167 for 13 pages of supplementary material. Order from ASIS/NAPS, Microfiche Publications, P.O. Box 3513 Grand Central Station, New York, NY 10163. Remit in advance \$4.00 for microfiche copy or for photocopy, \$7.75 up to 20 pages plus \$.30 for each additional page. All orders must be prepaid. Institutions and Organizations may order by purchase order. However, there is a billing and handling charge for this service of \$15. Foreign orders add \$4.50 for postage and handling, for the first 20 pages, and \$1.00 for additional 10 pages of material. \$1.50 for postage of any microfiche orders.

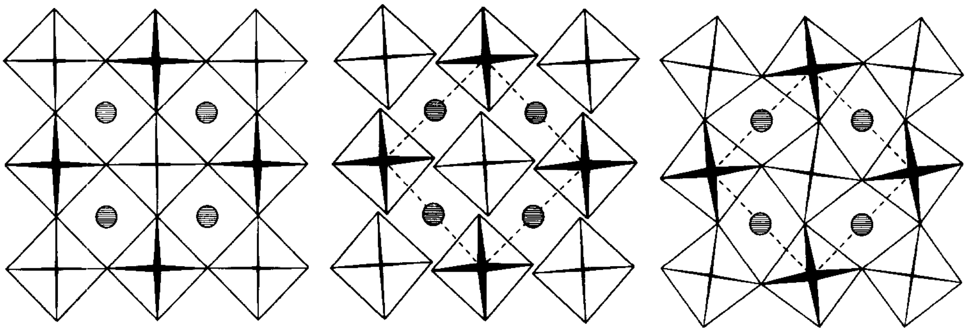

FIG. 4. The cubic K_2PtCl_6-type structure (left) and its tetragonally distorted substructures in a projection along the fourfold axis: *I*4/*m* ferrorotative β-Rb_2TeBr_6-type (middle) and *P*4/*mnc* antiferrorotative β-Rb_2TeI_6-type (right). The dotted lines show the *a*/*b* plane of the tetragonal unit cells. Different heights of the octahedra are given by different strokes.

this distances decrease again as a result of the more efficient packing. At 12.5 K the Br–Br distance between anions is more than 0.1 Å smaller than this distance within the anion. The rigid Te–Br bond (mean 2.700(4) Å from this three determinations) prevents a closer packing of the Br-atoms. The coordination of Rb by Br changes from a 12-fold (*Fm*3*m*) to a 4 + 4 + 4 (*I*4/*m*) one, while the (mean) distances Rb–Br are decreasing from 298 to 12.5 K.

This Γ-point condensation of a rotary phonon found for the phase transition of Rb_2TeBr_6 seems to be an exception among the simple compounds A_2TeBr_6 with an antifluorite arrangement of cations and anions. As reported in the introductional section of this paper a *X* point condensation seems to be the usual case, realized by an exchange of the alkali or halogen position in Rb_2TeBr_6 choosing a lighter or heavier atom (K_2TeBr_6, Rb_2TeI_6, for example). Figure 4 shows the cubic K_2PtCl_6 type structure and its tetragonal substructures in a projection along the fourfold axis. The group–subgroup relationship of the spacegroups (*21*) indicates the symmetry reduction:

$$\begin{tikzcd}
F\frac{4}{m}\bar{3}\frac{2}{m} \arrow[r, "t3"] & I\frac{4}{m}\frac{2}{m}\frac{2}{m} \arrow[r, "t2"] \arrow[rr, bend left, "k2"] & I\frac{4}{m} & P\frac{4}{m}\frac{2_1}{n}\frac{2}{c} \\
K_2PtCl_6 & & \beta\text{-}Rb_2TeBr_6 & \beta\text{-}Rb_2TeI_6 \\
\alpha\text{-}Rb_2TeBr_6 & & & \\
\alpha\text{-}Rb_2TeI_6 & & &
\end{tikzcd}$$

The order parameter for this second-order phase transition is the squared frequency of the softening $T_{1g}(\Gamma)$ rotation mode (*22*). To understand the behavior in this compound and to compare it with the phase transitions in related materials (e.g.,

Rb_2TeI_6, K_2SnCl_6) we calculated the phonon dispersion curves with the rigid ion model for the high-temperature $Fm3m$ phase.

Starting with the atomic force constants given by O'Leary and Wheeler for K_2ReCl_6 (*23*) the changes in the phonon frequencies were investigated by varying the force- and charge parameters. Similar calculations for K_2OsCl_6 are reported by Sutton *et al.* (*24*).

It was one surprising result that the rotational mode energies at the zone center (Γ) are always lower than these at the zone edge (X). The phase transition observed in Rb_2TeBr_6 ($Fm3m - I4/m$) thus agrees with the rigid ion prediction, in contrast to the antiferrorotative distortion of the octahedra in Rb_2TeI_6 ($Fm3m - P4/mnc$).

Evidently the limits of the model are exceeded with increasing radii of the anions or decreasing radii of the cations, respectively. The point charge model in the rigid ion calculation is a too rough approximation for the bigger ions, because there is no account of the polarization between shell and nucleus. Nevertheless the structure $I4/m$ indeed seems to be the more stable one, because we know no example of an A_2MX_6 compound in which the $P4/mnc$-structure remains stable when the temperature is further lowered.

References

1. R. J. Gillespie and R. S. Nyholm, *Quart. Rev. (London)* **11,** 339 (1957).
2. I. D. Brown, *Canad. J. Chem.* **42,** 2758 (1964).
3. A. K. Das and I. D. Brown, *Canad. J. Chem.* **44,** 939 (1966).
4. R. W. Berg and K. Nielsen, *Acta Chem. Scand. A* **33,** 157 (1979).
5. W. Abriel, *Z. Kristallogr.* **159,** 1 (1982).
6. D'Ans Lax, "Taschenbuch für Chemiker und Physiker," Vol. III, Springer-Verlag, Berlin (1970).
7. J. Ihringer, *Acta Crystallogr. Sect. A* **36,** 89 (1980).
8. W. Abriel, *Mater. Res. Bull.* **18,** 1419 (1983).
9. A. K. Das and I. D. Brown, *Canad. J. Chem.* **47,** 4288 (1969).
10. W. Abriel, Habilitationsschrift, Universität Marburg (1983).
11. W. Abriel, *Mater. Res. Bull.* **17,** 1341 (1982).
12. J. Ihringer, *Solid State Commun.* **41,** 525 (1982).
13. G. M. Sheldrick, *in* "Computing in Crystallography," p. 34, Delft Univ. Press (1978).
14. "International Tables for X-Ray Crystallography," Vol. IV, Kynoch Press, Birmingham (1974).
15. D. T. Cromer and D. Libermann, *J. Chem. Phys.* **53,** 1891 (1970).
16. J. Ihringer, *J. Appl. Crystallogr.* **15,** 1 (1982).
17. R. A. Young, P. E. Mackie, and R. B. von Dreele, *J. Appl. Crystallogr.* **10,** 262 (1977).
18. V. Schomaker and K. N. Trueblood, *Acta Crystallogr. Sect. B* **24,** 63 (1968).
19. P. Roberts and G. M. Sheldrick, unpublished.
20. M. Sutton and R. L. Armstrong, *Phys. Rev. B* **25,** 1813 (1982).
21. Th. Hahn, Ed., "International Tables for Crystallography, Vol. A," Reidel, Dordrecht and Boston (1983).
22. E. J. Veenendahl, H. B. Brom, and J. Ihringer, *Physica B* **114,** 31 (1982).
23. G. P. O'Leary and R. G. Wheeler, *Phys. Rev. B* **1,** 4409 (1970).
24. M. Sutton, R. L. Armstrong, B. M. Powell, and W. J. L. Buyers, *Phys. Rev. B* **27,** 380 (1983).